

Using the Ising Model to Describe Resonance Scattering

A thesis submitted in partial fulfillment of the requirement for
the degree of Bachelor of Science in Physics from
The College of William and Mary

by

Andrew D. Favaloro

Accepted for: B.S. in Physics

Advisor: Prof. Konstantinos Orginos

Prof. Gina L. Hoatson

Williamsburg, Virginia
May 2009

Contents

Acknowledgments	ii
List of Figures	iv
Abstract	v
1 Introduction	1
2 Scattering and the Scattering Phase Shift	2
3 The Simulation	5
3.1 The Ising Model	5
3.2 Coupled Ising Fields	7
3.3 Update Algorithm	7
3.4 Simulation Specifics	8
4 Data Analysis	12
4.1 Two-Point Function	12
4.2 Momenta and the Fourier Transform	13
4.3 Four-Point Functions and the Generalized Eigenvalue Problem	14
4.4 Code Specific Optimizations	16
5 Results	18
5.1 Masses	18
5.2 Other Energy Levels	19
6 Conclusion	22

Acknowledgments

I would like to thank Professor Orginos for his invaluable help in this project. The material has been complicated at times, and tedious at others, and his unending insight and patience has sought to resolve both of these problems. I would also like to thank the entire department of Physics at the College of William and Mary for all that they have taught me, in and out of the classroom, as well as presenting me with the opportunity to do research, which has been an intensely rewarding experience. Finally, I would like to thank professor Hoatson for pushing the researching Seniors as hard as she has.

List of Figures

2.1	A graph showing the roots of the quantization condition. Note how quickly the blue curve $\left(\frac{V_0 m}{\hbar^2 k}\right)$ approaches 0, and intersects with the red curve $(\tan(kL))$ in evenly spaced intervals of $\frac{n\pi}{L}$. Each point of intersection is $(k, \delta_l(k))$	3
3.1	A plot of the magnetization of a 4-Dimensional lattice for varying coupling constants κ . There exists a second order phase transition at approximately $\kappa = 0.735$. Around this point, the curve seems to smoothly curve upwards instead of sharply increase as is the case of second order phase transitions - this is due to finite volume corrections. As the volume increases, the phase transition becomes more sharp.	6
3.2	Plots showing various analyses of simulation data, where each color represents a different value of g . The first picture shows the magnetization as a function of simulation time. Note that relatively quickly, within the first 100s of updates, the magnetization reaches its steady state. It approaches that value so quickly that the standard deviation, plotted in the second picture, which only uses 2000 data points at a time, looks discontinuous at thermalization. The Autocorrelations show how, for differing values of g (red: $g=0.004$, green : $g=0.008$, blue: $g=0.010$, violet, $g=0.016$), statistically independent configurations are further spaced apart.	9
3.3	These plots show the masses of the ϕ (the red lines) and ρ (the green lines). particles as functions of the coupling constants κ_ϕ and κ_ρ , and g . Respectively. Unless otherwise being varied, the parameters are $\kappa_\phi = 0.07325, \kappa_\rho = 0.0718, g = 0.008$. Note that in the κ_ρ plot, the ρ reaches a maximum around 0.0718, and decreases monotonically outwards from that point, while the ϕ mass remains constant. In the ϕ plot, note that the ϕ mass increases as a function of κ_ϕ . Both of these reflect that there is a critical value of the κ parameter, which creates the maximum possible mass: in the case of κ_ρ , it is approximately 0.07184, and for κ_ϕ , it is greater than 0.0738	11

4.1	This figure shows a good two-point function on a logarithmic scale. Note that, until approximately $t = 10$, the data points fall into straight diagonal lines - this show a clean signal of e^{-mt} , where m is the slope of this line, which is the best fit we can make. The region where the plot is disconnected is the region in which the two-point function is 0 within statistical error, and crossed into negatives. The abnormal shape of this graph is a product of periodic boundary conditions : Here, $t = 30$ is just the same as $t = 2$: when running fitting programs, we account for this by trying to fit a function of the form $e^{-mt} + e^{-m(t_{max}-t)}$. . .	13
4.2	A figure taken from the Rommukainen and Gottlieb[6] paper on the same topic plotting energy versus length. Notice how the second energy level is decaying, plateauing, and then decaying again, right when the third level starts to plateau. The decaying energy levels fall as, approximately, $E_n = 2\sqrt{m^2 + p_n^2}$, the non-interacting energy levels. The value where the second and third energies represents a bound state of sorts, corresponding to the creation of a resonant particle.	15
5.1	Plots of the two masses as a function of length. The erratic behavior of the ρ particle (green) as compared to the relatively constant mass of the ϕ (red) suggests that this data should be re-evaluated.	20
5.2	This shows the two-point function for $L = 12$. Notice that even though the error bars on every point are very small, suggesting that the data is “correct”, the two-point function is too rounded at its bottom, and not flat enough to extract a good exponential fit. Though it is harder to tell by inspection, it also seems that the decay is also not exponential. The rounded nature of this graph has to do with “interactions felt around the world” : That is, because of the periodic boundary conditions on time, the signal is interfering with itself too much to get a good exponential fit.	20
5.3	The non-interacting energy levels $E_n = 2\sqrt{m_\phi^2 + p_n^2}$ are plotted in black, corresponding to $p_n^2 = 0, 1, 2, 3$ from the bottom down. The energy levels are plotted as functions of length. As you can see, several of the calculated energy levels match very closely non-interacting energy levels, as would be expected. Here	21

Abstract

This thesis sets out to create a model with which we can further examine resonance scattering. Many of the techniques used are well established within the community of Lattice Quantum Chromodynamics and other field theories. However, the value of the thesis is in being able to build them for a model system. We begin by discussing the theory behind the project, namely the phenomenon of resonance scattering. We then discuss some of the details of our simulation. We then discuss the manner in which the model relates to physical realities, and finally discuss some of our results and conclusion.

Chapter 1

Introduction

While Quantum Chromodynamics can calculate the masses of stable hadrons, effectively modeling the nature of unstable particles has always been a challenge. For instance, the ρ meson, which has a mean lifetime of 4.4×10^{-24} s, appears as a resonance in the elastic $\pi\pi \rightarrow \pi\pi$ scattering in the angular momentum $l = 1$ and isospin $I = 1$ channel. Due to their unstable nature, these particles themselves are hard to study, but by studying the interactions ($\pi\pi \rightarrow \pi\pi$) we can glean information about its resonances (ρ).[6]

This paper establishes a computational method of modeling such a decay using a statistical system, the Ising Model. The ideas are not new : this particular model has been used in the past to study the exact same structure. However, we explore the use of new update algorithms so as to achieve more efficiency in the computation. Moreover, emulating previous work like this provides a mechanism to check our work along the way.

Chapter 2

Scattering and the Scattering Phase Shift

In this section, I will discuss the effects of finite volume scattering with a simple example. Consider a particle with wavefunction φ in torus of circumference $2L$, with a potential of $V(x) = V_0\delta(x)$. This can be considered a one-dimensional problem with the restriction that $\varphi(L) = \varphi(-L)$. Upon further inspection, we can deduce several other properties of this wavefunction. Firstly, because $V(x)$ is even, we can take the wavefunction to be even. This implies that its derivative, $\frac{d\varphi}{dx}$ must be odd. By the continuity of the wavefunction and its derivative, we see that at $\frac{d\varphi}{dx}\Big|_{(L)} = \frac{d\varphi}{dx}\Big|_{(-L)} = 0$. Finally, we note that because of the infinite potential at $x = 0$, that the derivative need not be continuous there.

Taking all of these considerations about the qualities of the wave function into consideration, we write down the Schrödinger equation for this problem:

$$\left(-\frac{\hbar^2}{2m}\frac{d^2}{dx^2} + V_0\delta(x)\right)\varphi = E\varphi \quad (2.1)$$

Aside from Dirac Delta, this is the equation for a free particle. As an ansatz, we suggest that the solution to this equation is

$$\varphi(x) = e^{ik|x|} + e^{-ik|x|+2i\delta_l}. \quad (2.2)$$

We arrived at this result by taking the solution for a free particle, and modifying it to meet our stipulations. The substitution of $x \rightarrow |x|$ covers our symmetry condition, while the phase shift $2\delta_l$ on the second term is added because of potential difficulties resolving the boundary conditions.

The energy eigenvalues are easy to evaluate: we simply take the second derivative of φ at any point $x \neq 0$, in order to solve the Schrödinger equation for E . When calculated, they are clearly $\frac{k^2\hbar^2}{2m}$. We now turn our attention to solving for δ_l .

By our boundary conditions, we know $\left. \frac{d\varphi}{dx} \right|_L = ik(e^{ikL} - e^{-ikL+2i\delta_l}) = 0$. This resolves to $e^{ikL} = e^{-ikL+2i\delta_l}$, or $\delta_l = kL + n\pi$ for integer n .

We can also integrate the Schrödinger equation, such that $\lim_{\varepsilon \rightarrow 0} \int_{-\varepsilon}^{\varepsilon} \left[E + \frac{\hbar^2}{2m} \frac{d^2}{dx^2} \right] \varphi dx = \int_{-\varepsilon}^{\varepsilon} V_0 \delta(x) \varphi dx$. After some rather trivial integration, we arrive at the result [5]

$$\frac{V_0 m}{\hbar^2 k} = \tan(kL) \quad (2.3)$$

Much like a finite potential well, we find a transcendental equation relates to us the bound states. However, unlike a finite potential well, we infinitely many bound states, as the two functions intersect infinitely many times. Furthermore, as k increases, the left hand side approaches 0, and the quantization condition becomes $0 = \tan(kL)$, which has solutions $k_n = \frac{n\pi}{L}$. Thus, for large n , $k_n \approx \frac{n\pi}{L}$. As a final note of curiosity, we note that for large L , the spacing between momentum levels approaches 0. Thus, we see that for small L and large n , the energy levels approach $E_n = \frac{\hbar^2 n^2 \pi^2}{2mL^2}$, the energy levels of the infinite square well. For large L and small n , we see that the energy levels are very close to each other, and approach the continuous energy spectrum of a free particle.

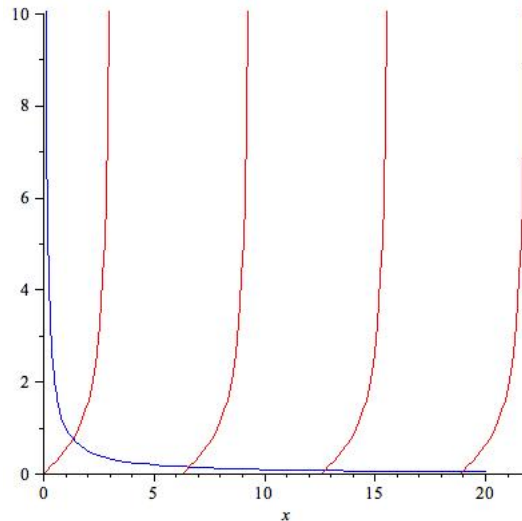


Figure 2.1: A graph showing the roots of the quantization condition. Note how quickly the blue curve $\left(\frac{V_0 m}{\hbar^2 k} \right)$ approaches 0, and intersects with the red curve ($\tan(kL)$) in evenly spaced intervals of $\frac{n\pi}{L}$. Each point of intersection is $(k, \delta_l(k))$

This section has demonstrated the effect that finite volumes (in this case, lengths) can have on scattering processes. More importantly, the calculation of δ_l , the scattering phase shift, can give insight into several different key aspects of the scattering process.

Chapter 3

The Simulation

3.1 The Ising Model

The Ising Model is a lattice system, which has been extensively used to describe magnetism, among other phenomena. The model creates a lattice in N dimensions, at each point of which is a quantity called the Spin. According to the model, the spin at a location can only be either pointing up (with an associated value of $+1$), or pointing down (with an associated value of -1). We define the action of a single Ising Field to be [2]

$$S = -\kappa \sum_{\vec{x}, \hat{\mu}} \phi_{\vec{x}} \phi_{\vec{x}+\hat{\mu}} \quad (3.1)$$

where κ is a coupling parameter, restricted in our case to be positive, \vec{x} is an N -dimensional position on the lattice, $\hat{\mu}$ is a unit vector pointing either positively or negatively in any direction ($\hat{\mu} \in \{\pm \hat{x}_1, \dots, \pm \hat{x}_N\}$) and $\phi_{\vec{x}}$ is the Spin at the position \vec{x} . Each term of the sum is either positive if the two neighboring spins are aligned ($\phi_{\vec{x}} = \phi_{\vec{x}+\hat{\mu}}$), or negative if the two spins are anti-aligned ($\phi_{\vec{x}} = -\phi_{\vec{x}+\hat{\mu}}$). Thus, the action tends to a more negative number when spins are mostly aligned, towards a more positive number when the spins are mostly anti-aligned, and towards 0 when the spins are randomly distributed between the two.

We can also associate an energy with each spin as the sum of each nearest neighbor of that spin: that is, [2]

$$E(\phi_{\vec{x}}) = -2\kappa \sum_{\hat{\mu}} \phi_{\vec{x}+\hat{\mu}} \quad (3.2)$$

The factor of two is motivated by the fact that, strictly speaking, $\phi_{\vec{x}}$ occurs in the terms $\phi_{\vec{x}}\phi_{\vec{x}+\hat{\mu}}$ and $\phi_{\vec{x}-\hat{\mu}}\phi_{\vec{x}}$; however, because we sum over positive and negative unit vectors $\hat{\mu}$, these two terms are identical. In terms of thermodynamics, we can construct a Boltzmann factor around this energy, and establish that the probability of a particular spin being oriented upwards is

$$P(\phi_{\vec{x}} = 1) = \frac{e^{-E(\phi_{\vec{x}})}}{e^{E(\phi_{\vec{x}})} + e^{-E(\phi_{\vec{x}})}} \quad (3.3)$$

An interesting feature of the Ising Model (when $N > 1$) is a transition from an ordered phase to a disordered phase.[2] That is, there is a stable “Thermalized” state of the lattice, which occurs when the lattice reaches thermal equilibrium with itself. In which the expected value of the average spin (the Magnetization) is constant, no matter how many more updates are performed on the lattice. For low enough values of the coupling constant, the magnetization thermalizes to approximately 0 (within statistical error). After a critical coupling constant, though, the lattice thermalizes to non-zero values. In fact, at the critical value of κ , the average spin (the Magnetization of the Lattice) undergoes a second-order phase transition. (Fig. 3.1)

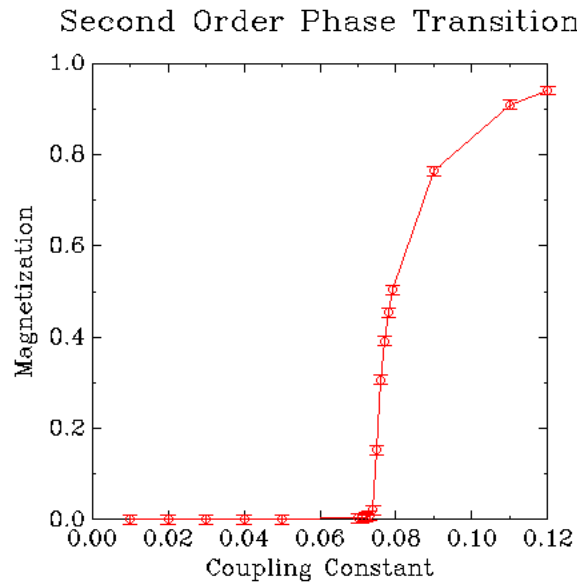


Figure 3.1: A plot of the magnetization of a 4-Dimensional lattice for varying coupling constants κ . There exists a second order phase transition at approximately $\kappa = 0.735$. Around this point, the curve seems to smoothly curve upwards instead of sharply increase as is the case of second order phase transitions - this is due to finite volume corrections. As the volume increases, the phase transition becomes more sharp.

3.2 Coupled Ising Fields

For the purposes of our experiment, we created two separate Ising fields (ϕ and ρ), coupled to each other. We defined the action to be [6]

$$S = g \sum_{\vec{x}, \hat{\mu}} \rho_{\vec{x}} \phi_{\vec{x}} \phi_{\vec{x}+\hat{\mu}} - \kappa_{\rho} \sum_{\vec{x}, \hat{\mu}} \rho_{\vec{x}} \rho_{\vec{x}+\hat{\mu}} - \kappa_{\phi} \sum_{\vec{x}, \hat{\mu}} \phi_{\vec{x}} \phi_{\vec{x}+\hat{\mu}} \quad (3.4)$$

where, as before, κ is a coupling constant for within one field (κ_{ϕ} for the ϕ field, and κ_{ρ} for the ρ field), while g is a coupling constant which governs the interaction each field has with each other. Note that in the case $g = 0$, the action is merely the sum of the action for two non-interacting Ising Fields.

As before, we can calculate the energy at each point of the fields, both the ϕ and the ρ . However, the consideration of the energy is slightly more complicated now due to the interaction between the two fields. We define the energy to be the sum of all terms in which that spin is involved divided by the value of the spin. That is,

$$E(\phi_{\vec{x}}) = \frac{1}{\phi_{\vec{x}}} \left(g \sum_{\hat{\mu}} \rho_{\vec{x}} \phi_{\vec{x}} \phi_{\vec{x}+\hat{\mu}} + g \sum_{\hat{\mu}} \rho_{\vec{x}-\hat{\mu}} \phi_{\vec{x}-\hat{\mu}} \phi_{\vec{x}} - 2\kappa_{\phi} \sum_{\hat{\mu}} \phi_{\vec{x}} \phi_{\vec{x}+\hat{\mu}} \right) = \quad (3.5)$$

$$g \sum_{\hat{\mu}} \phi_{\vec{x}+\hat{\mu}} (\rho_{\vec{x}} + \rho_{\vec{x}+\hat{\mu}}) - 2\kappa_{\phi} \sum_{\hat{\mu}} \phi_{\vec{x}+\hat{\mu}}$$

$$E(\rho_{\vec{x}}) = \frac{1}{\rho_{\vec{x}}} \left(g \sum_{\hat{\mu}} \rho_{\vec{x}} \phi_{\vec{x}} \phi_{\vec{x}+\hat{\mu}} - 2\kappa_{\rho} \sum_{\hat{\mu}} \rho_{\vec{x}} \rho_{\vec{x}+\hat{\mu}} \right) = g \sum_{\hat{\mu}} \phi_{\vec{x}} \phi_{\vec{x}+\hat{\mu}} - 2\kappa_{\rho} \sum_{\hat{\mu}} \rho_{\vec{x}+\hat{\mu}} \quad (3.6)$$

As before, phase transitions still occur, but they are clearly dependent on all three parameters, g , κ_{ϕ} , and κ_{ρ} .

3.3 Update Algorithm

In the past, other Ising Models have used Cluster Algorithms[6, 5] or Metropolis Algorithms to update their fields, as it was deemed computationally more efficient. Generally speaking, the Metropolis algorithm is slow and inefficient for a models such as this one. The cluster algorithm has been used extensively, and is, on normal machines, the best that can be done. With recent advances in parallel computing and other technological advances, however, we have adopted a heat-bath algorithm. We calculate the quantity $P(3.3)$ at every point on the lattice, choose a random number r between 0 and 1, and if $r > P$, then we set the spin to $+1$. If $r < P$, we set it to -1 . We have found it to run relatively quickly, and uses very little computer-time. This algorithm exploits the power of parallel computing, and we expect there to be a significant increase in efficiency with it. Our Monte Carlo runs were done on the Cyclades cluster at William and Mary. The use of the QDP++ library developed by Jefferson Lab was instrumental to handling of the updates.

At every update time, perform two sweeps on a checkerboard pattern (that is, if any given spin is being updated, then all of its nearest neighbors are not being updated. Similarly, if any spin is not being updated, then all of its nearest neighbors are.) Because most quantities in the Ising Model depend solely on nearest neighbor interactions, this sweep pattern ensures that each update updates the entire field in accordance with the model.

It is important that we create statistically independent configurations before we begin to measure data. Because the lattice begins in a state that has nothing to do with the update algorithm, and thus the physics of the situation, we need a way to ensure that the lattice has successfully evolved away from initial condition, and has reached thermal equilibrium. This state (the thermalized state) happens relatively quickly, although one way to check is to watch the standard deviation of the magnetization of each field. For low values of Monte Carlo time, the standard deviation is typically high, as the values are changing sporadically with each passing update. As time passes, however, the fields approach a configuration independent of their starting states, the standard deviation levels off to a constant value, reflecting that the change from one configuration to the next is typically the same, indicating that a thermalized state has been reached.

It is important to know when the system has evolved from one state into another so that we can correlate independent states with. If we did not know how long this took, we would be essentially analyzing the same data multiple times over, and losing time on analysis without gaining anything in terms of statistics. We compute the auto-correlation of a field ϕ , given by

$$A(\tau) = \frac{\sum_{i=0}^{N-\tau} (\phi_i - \langle \phi \rangle) (\phi_{i+\tau} - \langle \phi \rangle)}{\left(\sum_{i=0}^N (\phi_i - \langle \phi \rangle) \right)^2} \quad (3.7)$$

where ϕ_i is the magnetization of the lattice at monte carlo time i , and N is a sufficiently large number of configurations. This function decays exponentially, and when $A(\tau) \approx 0$ (within statistical noise), then we know that configurations τ apart are statistically independent.

3.4 Simulation Specifics

We use two coupled Ising fields to describe two separate particles, named ϕ and ρ for no substantial reason, which interact in a resonant reaction (that is, $\phi\phi \rightarrow \rho \rightarrow \phi\phi$). We construct an Ising field in four dimensions: three spatial dimensions, and one Wick-rotated time dimension. That is, the dimension we call t in our simulations actually represents $-it$. In this way, our t stands on equal footing with the other

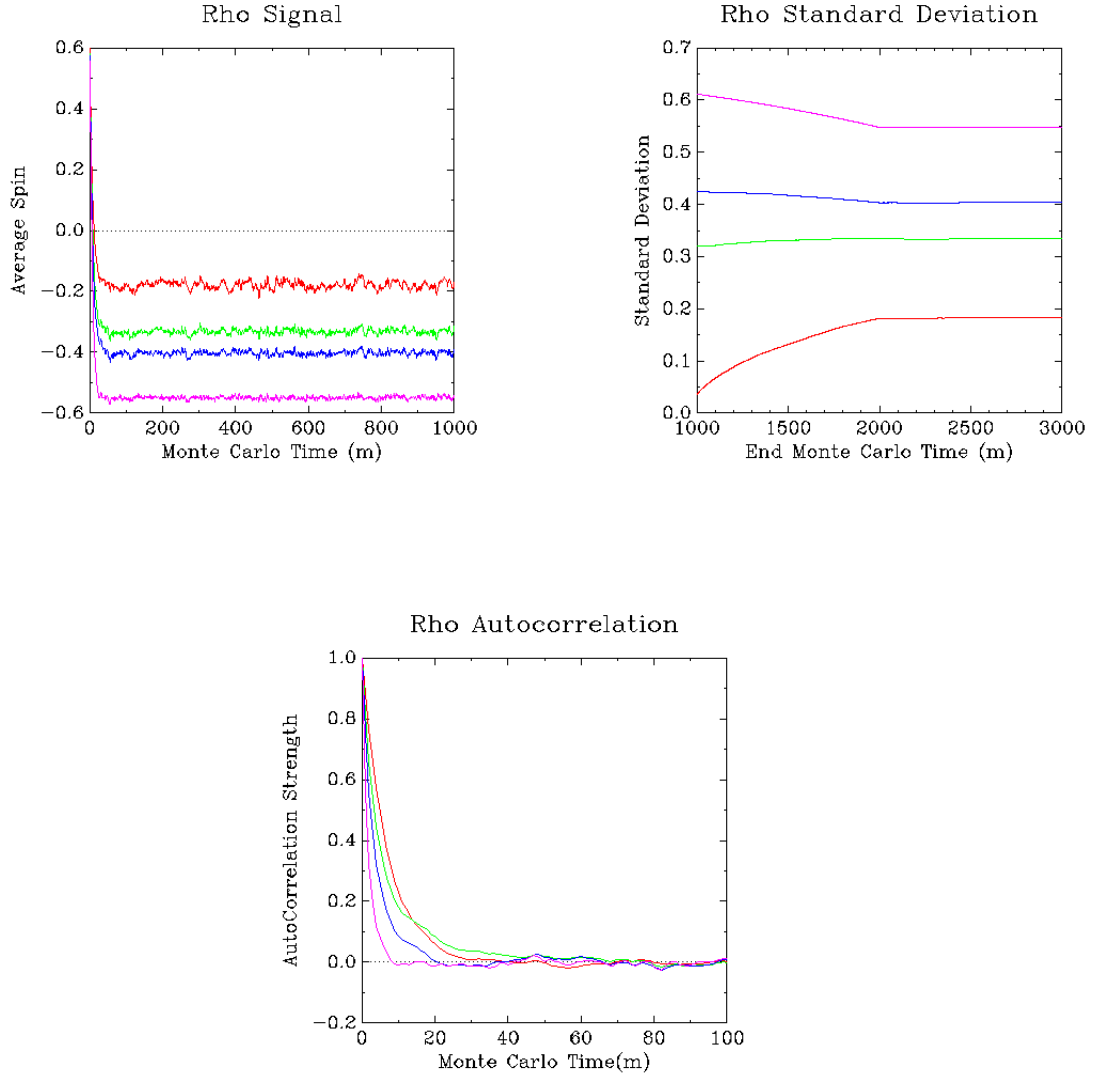


Figure 3.2: Plots showing various analyses of simulation data, where each color represents a different value of g . The first picture shows the magnetization as a function of simulation time. Note that relatively quickly, within the first 100s of updates, the magnetization reaches its steady state. It approaches that value so quickly that the standard deviation, plotted in the second picture, which only uses 2000 data points at a time, looks discontinuous at thermalization. The Autocorrelations show how, for differing values of g (red: $g=0.004$, green: $g=0.008$, blue: $g=0.010$, violet, $g=0.016$), statistically independent configurations are further spaced apart.

Euclidean dimensions, and a four dimensional model as described is justified. The main difference this makes in terms of any substantial results is that several key calculations turn out to be sums of exponentials: in actual space, they are oscillatory functions, with frequencies related to the decay widths we calculate. The dimension we designate to be time is, in a sense, arbitrary: we could just as easily do all of our analysis in the z direction instead of in the t direction. However, to distinguish the temporal dimension from the spatial ones, as well as to have enough temporal length to extract good exponential fits, we construct lattices that have dimensions $n \times n \times 2n$, giving the temporal dimension twice the length of all the spatial ones.

Though we calculate the Ising field at every point (x, y, z, t) on the grid, the only data we record at any given update is the spatial average of the spins on any given timeslice.

The action described in eq. 3.4 was not chosen completely arbitrarily. It is chosen to resemble two interacting fields as given in Quantum Chromodynamics, particularly the ϕ^4 theory, defined by the action[6]

$$S = \int d^4x \left(\frac{1}{2} \partial^\mu \phi \partial_\mu \phi + \frac{1}{2} m_{\phi,0}^2 \phi^2 + \frac{\lambda_{\phi,0}}{4!} \phi^4 + \frac{1}{2} \partial^\mu \rho \partial_\mu \rho + \frac{1}{2} m_{\rho,0}^2 \rho^2 + \frac{\lambda_{\rho,0}}{4!} \rho^4 + \frac{g_0}{2} \rho \phi^2 \right) \quad (3.8)$$

where ϕ, ρ are the fields and particles in question, $m_{\phi,0}, m_{\rho,0}$ are the groundstate masses of the particles, $\lambda_{\phi,0}, \lambda_{\rho,0}$ are scaling constants, and g_0 is a coupling constant which defines the strength of the interaction between the ρ and $\phi\phi$ states. In comparing eq. 3.4 with eq. 3.8, we can see a relationship between the mass parameters and the κ parameters, as well as a correlation between g_0 and g . Thus, we can expect that the κ parameters be related to the masses of the particles, while the g parameter dictates how strongly the two interact: in both cases, the presence of one ρ and two ϕ (whether the value for ϕ be squared or taken from two different points on the lattice) indicates that the ρ particle can decay into two ϕ 's. This shows that eq. 3.4 is a discretized version of 3.8, adapted for the ising model.

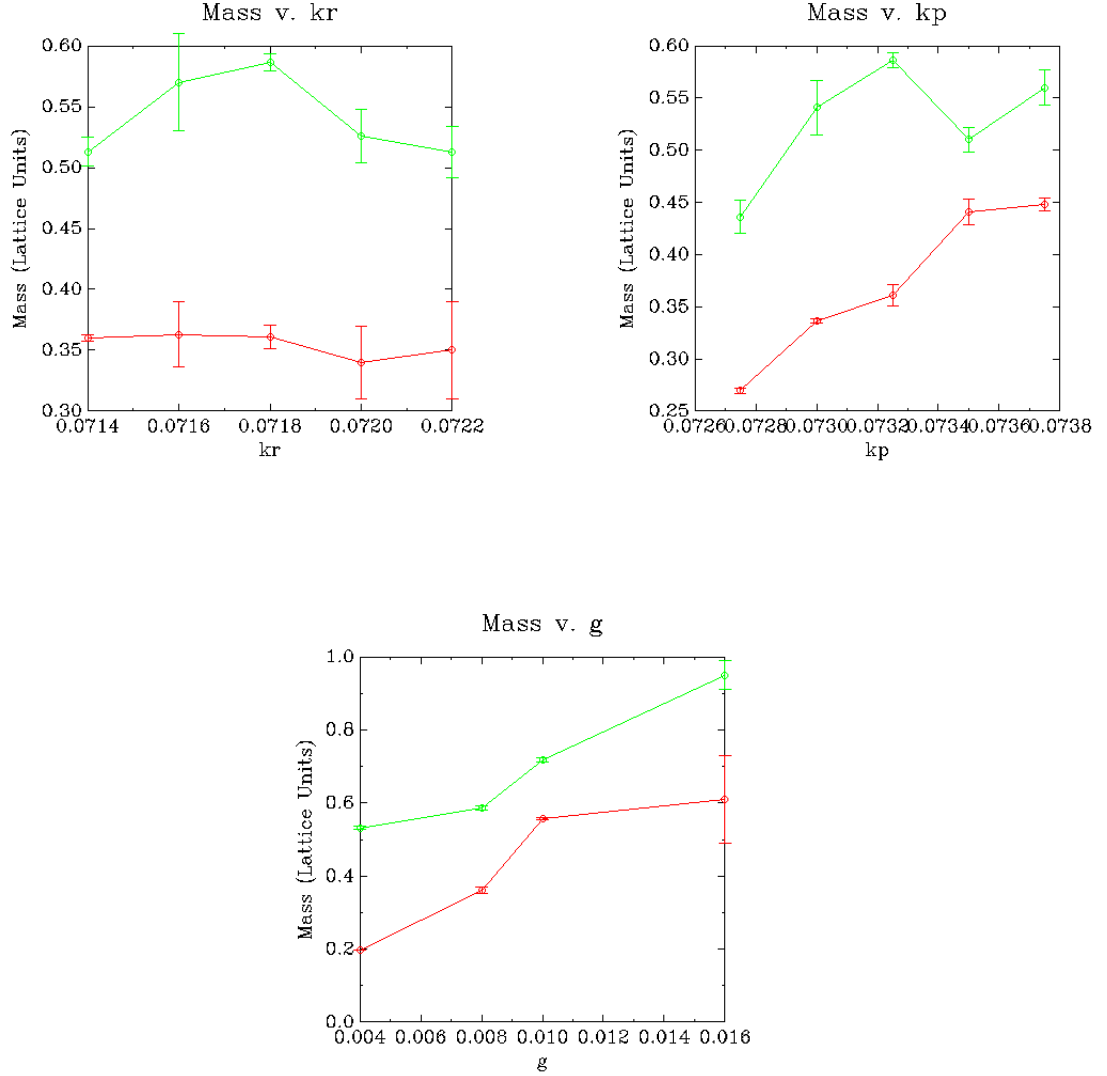


Figure 3.3: These plots show the masses of the ϕ (the red lines) and ρ (the green lines) particles as functions of the coupling constants κ_ϕ and κ_ρ , and g . Respectively. Unless otherwise being varied, the parameters are $\kappa_\phi = 0.07325$, $\kappa_\rho = 0.0718$, $g = 0.008$. Note that in the κ_ρ plot, the ρ reaches a maximum around 0.0718, and decreases monotonically outwards from that point, while the ϕ mass remains constant. In the ϕ plot, note that the ϕ mass increases as a function of κ_ϕ . Both of these reflect that there is a critical value of the κ parameter, which creates the maximum possible mass: in the case of κ_ρ , it is approximately 0.07184, and for κ_ϕ , it is greater than 0.0738

Chapter 4

Data Analysis

4.1 Two-Point Function

The two-point function is used to examine how similar a spin configuration is from one time-slice to another. This is useful to us because it answers the question of if one particular spin is flipped, what kind of a “spin wave” will propagate in the t direction on the lattice. To construct the two-point function mathematically, we use the formula[6]

$$C(t) = \langle (M(t) - \langle M(t) \rangle) (M(0) - \langle M(0) \rangle) \rangle \quad (4.1)$$

Upon analyzing the two-point function, we notice that it takes the form of an exponential decay with time. Such a result is expected, as the two-point function also takes the form[6]

$$C(t) = \sum_n A_n e^{-E_n t} \quad (4.2)$$

where A_n are amplitudes which depend on the energy levels, and E_n are the energy levels themselves. Ideally, if we could fit the two-point function perfectly, we could extract all of the energy levels of this system to exquisite detail. Unfortunately, this is not possible.

Equation 4.2 is essentially a correlation amplitude[7]. The correlation function represents a transition amplitude : that is, the probability that a particle will remain in a given state after a given amount of time. According to Sakurai, we find that the propagator $C(t)$ is related to the Hamiltonian of the system by[7]

$$C(t) = \langle \alpha | e^{-\frac{i}{\hbar} \hat{H} t} | \alpha \rangle \quad (4.3)$$

Where H is the Hamiltonian operator, and α is a linear combination of energy eigenstates $\left(|\alpha\rangle = \sum_{a'} c_{a'} |a'\rangle \right)$. This can be reduced, in Minkowski space, to be [7]

$$C(t) = \sum_{a'} |c_{a'}|^2 \exp\left(\frac{-iE_{a'} t}{\hbar}\right) \quad (4.4)$$

After Wick-rotating the time from t to it , and applying fundamental units ($\hbar \equiv 1$), we arrive at equation 4.2, as expected.

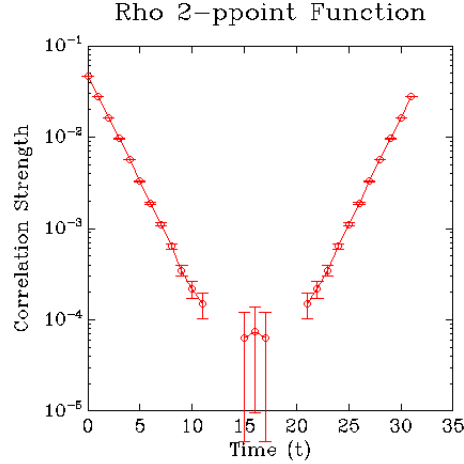


Figure 4.1: This figure shows a good two-point function on a logarithmic scale. Note that, until approximately $t = 10$, the data points fall into straight diagonal lines - this shows a clean signal of e^{-mt} , where m is the slope of this line, which is the best fit we can make. The region where the plot is disconnected is the region in which the two-point function is 0 within statistical error, and crossed into negatives. The abnormal shape of this graph is a product of periodic boundary conditions: Here, $t = 30$ is just the same as $t = 2$: when running fitting programs, we account for this by trying to fit a function of the form $e^{-mt} + e^{-m(t_{max}-t)}$

Making the ansatz that the ground state energy E_0 (corresponding to $\vec{p} = 0$) is the smallest of these energies, and thus contributing the most significantly at large times, we can assume that all other energy levels contribute negligibly, fit the two-point function at long times, and extract the masses out of two-point function. However, the signal is often clouded by the other energy levels, and hence, a simple two-point function on its own can only give a rough estimate of the ground state energy, and no insight into the other energy levels.

4.2 Momenta and the Fourier Transform

The quantization condition established on the lattice requires that all momenta \vec{p} take the form

$$\vec{p} = \frac{2\pi}{L}\vec{n}, \vec{n} \in \mathbb{Z}^3 \quad (4.5)$$

We can use this information to apply a Fourier Transform to the spins of the both the ϕ and the ρ Ising fields according to[6]

$$\tilde{\phi}_{\vec{x}}(\vec{p}, t) = \sum_{\vec{x}} e^{i(\vec{p}\cdot\vec{x})} \phi(\vec{x}, t) \quad (4.6)$$

We know, from special relativity, that the energy states of the $\phi\phi$ that we have placed in this box are

$$E_n = 2\sqrt{m_\phi^2 + p_n^2} \quad (4.7)$$

where m_ϕ is the mass of the ϕ particle, and p_n is given in equation 4.5. The factor of 2 arises from the fact that there are two interacting ϕ particles bouncing around in the box, each with opposite momenta (because there is 0 net momentum), so they each have the same value of p_n^2 .

From here, as before, we can take the fourier transform of just a timeslice, by averaging over all \vec{x} . Because we care so frequently about the fields on just one timeslice at a time, we often lose track of the true nature of the spins on that timeslice. For instance, we may be able to extrapolate how many spins are pointing up and pointing down, but where are they in relation to each other? How are they arranged? The Fourier Transform allows us to gain better insight into the layout of such a system by creating an explicit dependence of x in our observable ; in theory, using information from all L^3 possible Fourier Transforms could uniquely determine the configuration of the lattice.

More importantly, the Fourier Transform allows us to shift the ϕ s into a frame in which they are moving. This allows us to study more general forms of decay, though we must stay in the zero-momentum center of mass frame. This also allows us to see more clearly the entire energy spectrum of the $\phi\phi$ part of the interaction, which can give us good insight into the energy spectrum of the ρ particle. Because we are considering only the center of mass frame, the ρ will always have no momentum, and this method of Fourier Transform is invalid. However, if we examine the energy levels of the ϕ as a function of length, we can expect to see a phenomenon called ‘‘Avoided Energy Level Crossing’’ where in the energy levels of ϕ decrease exponentially as a function of L , except to plateau at energy levels of the ρ . This point represents the case of resonance that we have been expecting to study (see fig 4.2).

4.3 Four-Point Functions and the Generalized Eigenvalue Problem

In order to analyze the energy levels taken from the fourier transformed lattice, we need to construct a four point function which connects the possible states of the interaction : either two ϕ s with equal and opposite momenta or a single ρ with 0 momentum. We construct the function[6]

$$C_{ij}(t) = \left\langle \left(\tilde{\phi}(\vec{p}_i, t) \tilde{\phi}(-\vec{p}_i, t) - \langle \tilde{\phi}(\vec{p}_i, t) \tilde{\phi}(-\vec{p}_i, t) \rangle \right) \right\rangle. \quad (4.8)$$

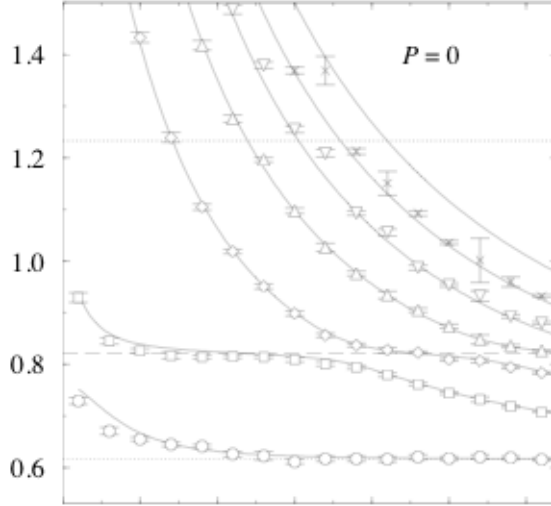


Figure 4.2: A figure taken from the Rommukainen and Gottlieb[6] paper on the same topic plotting energy versus length. Notice how the second energy level is decaying, plateauing, and then decaying again, right when the third level starts to plateau. The decaying energy levels fall as, approximately, $E_n = 2\sqrt{m^2 + p_n^2}$, the non-interacting energy levels. The value where the second and third energies represents a bound state of sorts, corresponding to the creation of a resonant particle.

$$\left(\tilde{\phi}(\vec{p}_j, 0) \tilde{\phi}(-\vec{p}_j, 0) - \langle \tilde{\phi}(\vec{p}_j, 0) \tilde{\phi}(-\vec{p}_j, 0) \rangle \right)$$

where the momenta \vec{p}_i have all been ordered in some arbitrary order, for the case of ϕ s elastically scattering. If we want to include a ρ , we would remove one term and replace it with $\tilde{\rho}(0, t)$ or $\tilde{\rho}(0, 0)$ as necessary. This matrix is, in the infinite statistics limit, real and symmetric.

To extract energy levels from this four point function, we need to consider the Generalized Eigenvalue problem, which is of the form

$$Au = \lambda Bu \quad (4.9)$$

In our case, we choose $A = C(t)$, $B = C(t_0)$, and $u(t, t_0), \lambda(t; t_0)$ to be arbitrary functions which solve the equation. In some very lucky cases, the answer is almost trivial: u and λ are the eivenvectors and eigenvalues of $C^{-1}(t_0)C(t)$. However, in the case where C is singular at time t_0 , this solution is invalid. The problem is still solvable in general though, especially if you make a few important assumptions

We can construct the correlation matrix $C(t)$ as

$$C(t) = \sum_n e^{-E_n t} |\psi_n\rangle \langle \psi_n| \quad (4.10)$$

where $|\psi_n\rangle_i = \sum_i \langle 0| \hat{O}^i |n\rangle$, where $|0\rangle, |n\rangle$ are Eigenstates of the Hamiltonian of

our system, \hat{O}^i projects the i^{th} momentum onto the state, and this is just the i^{th} component in some orthonormal basis. We now introduce the dual vectors $|u_n\rangle$ defined by $\langle u_n|\psi_m\rangle = \delta_{nm}$. Then we see that $C(t)|u_n\rangle = \left(\sum_{n'} e^{-E_{n'}t} |\psi_{n'}\rangle \langle \psi_{n'}|\right) |u_n\rangle = e^{-E_n t} |\psi_n\rangle$. Thus, [1]

$$C(t_0)|u_n\rangle = e^{-E_n t_0} |\psi_n\rangle = e^{-E_n(t_0-t)} e^{-E_n t} |\psi_n\rangle = e^{-E_n(t_0-t)} C(t)|u_n\rangle \quad (4.11)$$

Thus, the generalized eigenvalues are $e^{-E_n(t-t_0)}$, and the generalized eigenvectors are $|u_n\rangle$. Using the same fitting techniques that we've used to extract masses out of the two-point functions, we can extract these energy levels, and analyze them as necessary.

We would need to have all L^3 energy levels in order to properly get every eigenvalue out of this matrix. However, because the matrix is symmetric, we can exploit a feature of Hermitian matrices called eigenvalue interlacing. In a given $N \times N$ Hermitian matrix H , there are N , real eigenvalues, which can be ordered $\lambda_1 \leq \lambda_2 \leq \dots \leq \lambda_N$. If we were to consider any $N-1 \times N-1$ principal submatrix of H (H'), then again there are $N-1$ real eigenvalues which can be ordered $\lambda'_1 \leq \lambda'_2 \leq \lambda'_{N-1}$. Eigenvalue interlacing tells us that [4]

$$\lambda_1 \leq \lambda'_1 \leq \lambda_2 \leq \lambda'_2 \leq \dots \leq \lambda_{N-1} \leq \lambda'_{N-1} \leq \lambda_N \quad (4.12)$$

It can further be shown that in our Correlation function matrix, low momenta of the $\phi\phi$ state do not correlate highly to higher momenta. Thus, we can essentially consider the “lower momentum state matrix” to be embedded in the entire matrix $C(t)$, with eigenvalues determined almost solely by this embedded matrix. This is of course, not true, because in an $N' \times N'$ submatrix of an $N \times N$ matrix, the lower few may be uniquely determined by the $N' \times N'$ matrix, but state N' will clearly not be, as it is relatively strongly correlated to states outside of the matrix. Combining the notions of interlacing with this idea of embedded matrices, we can determine that even if there are L^3 energy states, we can get good signals on the first few, lowest states without having to measure every higher fourier transform.

4.4 Code Specific Optimizations

We made several optimizations within the code that reflect a need to speed up computer time and do not reflect important pieces of the theory. Firstly, because we are working in a 0 momentum frame for the purposes of this work, we recognize that

$$\tilde{\phi}(\vec{p}, t) \tilde{\phi}(-\vec{p}, t) = \left(\sum_{\vec{x}} e^{i(\vec{x}\cdot\vec{p})} \phi(x, t)\right) \left(\sum_{\vec{x}} e^{-i(\vec{x}\cdot\vec{p})} \phi(x, t)\right) = \left|\tilde{\phi}(p, t)\right| \quad (4.13)$$

For this reason, we only fourier transformed half of the non-zero momenta, choosing not to record the Fourier Transforms corresponding to negative momenta already

checked., and never recorded the complex value of the of the fourier transform, but only its absolute value. This reduced the run time of our program by approximately half.

Secondly, in the analysis stage of our regime, we averaged over rotated momenta (ie, $(1, 0, 0)$, $(0, 1, 0)$, $(0, 0, 1)$) in the construction of our correlation matrix. This reduced our analysis time by approximately half, although in the future for larger momenta spectrum, this optimization has the potential to reduce that time even further. By making this average, we can maintain the reduction we would otherwise have in statistics without having to construct a very large matrix with some rows / columns that are very similar to each other.

Finally, after some problems with memory management in the C++ programs we were using, we switched to Python scripts for most of our data retrieval and analysis. Python was significantly faster (one script finished in less than 15 minutes what it had taken the C++ program an entire day to do). A possible continuation of this work could be to combine these two to interface with each other, as C++ is certainly a more powerful language, or perhaps even fix some of memory management issues that the C++ programs were having.

Chapter 5

Results

5.1 Masses

Figure 3.4 shows some of the results we obtained for masses. The point of these plots was to probe how the different parameters we used in our model $(\kappa_\phi, \kappa_\rho, g)$ effected the masses. For the most part, these signals were relatively clean - there were typically only two strong exponentials that seemed to contribute to the decay of the two-point function. Clearly, with more time spent on running the program and collecting data, the one clear signal would prevail, and with higher statistics. However, as it stands, the two contributions were typically very distinct and, and it was easy to tell which was the correct signal. All these datasets come from a volume of length $L = 16$. These three plots reveal interesting facts about how the model works. For instance, in the plot of mass v. κ_ρ , we can see that there is a maximum mass of the ρ particle achieved at a value of $\kappa_\rho = 0.0718$. This shows the importance of the phase transition : We can expect the masses to be [3]

$$\frac{1}{m_0} \propto \xi \propto \frac{1}{|\kappa - \kappa_c|^\nu} \quad (5.1)$$

where κ_c is the κ value at which the phase transition occurs, ξ is the correlation length, defined by equation 5.1, and ν is a critical exponent, dependent on the nature of the system. Thus, we can expect that $\kappa_\rho = 0.0718$ is very close to the critical κ value and the point at which the phase transition occurs. We can also see that the mass of the ϕ increases as a function of κ_ϕ monotonically on the interval we plotted. This also fits into our model, and suggests that κ_c for the ϕ is outside of the range we plotted.

Slightly disconcerting within these two plots is the effect of the mass whose parameter is not being changed. In plotting mass v. κ_ρ , we see that the ϕ particle is relatively constant, reflecting that κ_ρ doesn't effect the mass of ϕ much. However, when we plot mass v. κ_ϕ , we see the ρ particle's mass changing erratically, and not even increasing or decreasing monotonically. The data seems to suggest that κ_ϕ is

significantly involved in the mass of ρ . To explore this some more, we want to investigate the one point at $\kappa_\phi = 0.0735$ where ρ 's mass decreases, as well as investigate some intermediary points on these plots.

Another thing I decided to check was how the mass of the particles was effected by spatial length. The results here are slightly erratic (fig 5.1), suggesting that we may need to re-examine the data. Part of the problem is that, though we ran the simulation on lengths less than $L = 14$, there was no stable way to extract a good exponential fit on these data sets. This is most likely due to “interactions around the world”, in which the periodic boundary conditions of our lattice have too much of an effect on each other, and lead to unreliable signals (fig 5.1).

5.2 Other Energy Levels

After finding a good fit for the mass, we then proceeded to turn our attention to plotting the other energy levels. Figure 5.3 shows the results from those finds, which were run with the parameters $\kappa_\phi = 0.07325, \kappa_\rho = 0.0718, g = 0.008$. We let each lattice run for approximately 800 computer hours, resulting in about 5600 hours of computer time being spent. However, because we could run the machine in parallel, this took only 200 hours in actual time.

When we began to plot the energy levels, however, it became apparent that something had gone awry. figure 5.3 shows the non-interacting energy levels in black, suggesting that the green data set (on the bottom) is the ground-state. What may have happened, then, is that the blue dataset below that set is the ρ particle. Because it is lighter than $\phi\phi$ (The green line corresponding to the ground state is, to accuracy of 94% or higher (depending on the length) twice the value determined by fitting the two-point function : the 6% margin of error is likely explainable by the interference of higher order energy levels in equation 4.2), there is no chance that it can occur as a resonance - in fact, it occurs in this simulation as a stable particle. Clearly, we need to go back and choose other parameters ($\kappa_\phi, \kappa_\rho, g$) such that the ρ mass is greater than twice the ϕ mass.

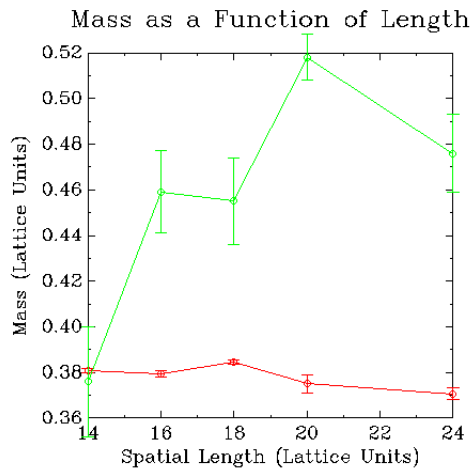


Figure 5.1: Plots of the two masses as a function of length. The erratic behavior of the ρ particle (green) as compared to the relatively constant mass of the ϕ (red) suggests that this data should be re-evaluated.

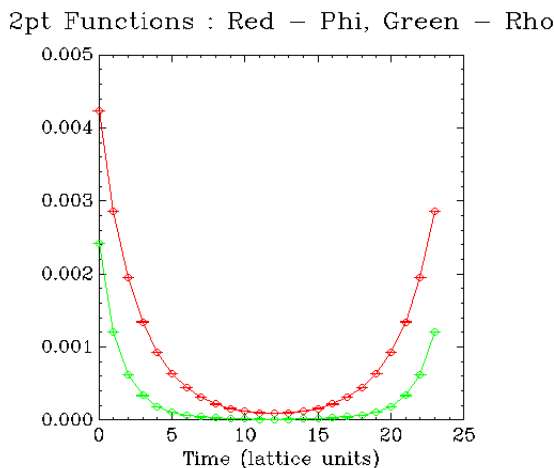


Figure 5.2: This shows the two-point function for $L = 12$. Notice that even though the error bars on every point are very small, suggesting that the data is “correct”, the two-point function is too rounded at its bottom, and not flat enough to extract a good exponential fit. Though it is harder to tell by inspection, it also seems that the decay is also not exponential. The rounded nature of this graph has to do with “interactions felt around the world” : That is, because of the periodic boundary conditions on time, the signal is interfering with itself too much to get a good exponential fit.

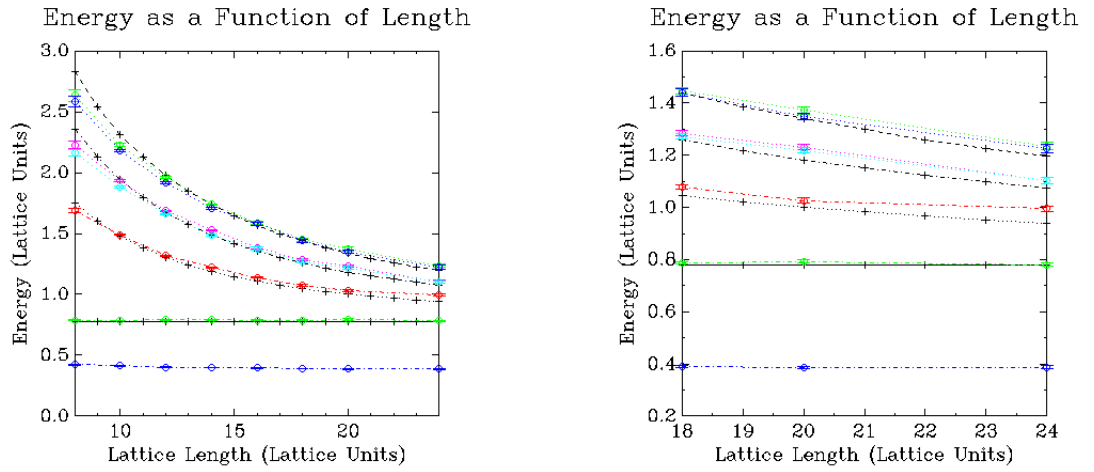


Figure 5.3: The non-interacting energy levels $E_n = 2\sqrt{m_\phi^2 + p_n^2}$ are plotted in black, corresponding to $p_n^2 = 0, 1, 2, 3$ from the bottom down. The energy levels are plotted as functions of length. As you can see, several of the calculated energy levels match very closely non-interacting energy levels, as would be expected. Here

Chapter 6

Conclusion

As it stands, this project can have no actionable conclusion - that is to say, we cannot say whether or not. Also, we would have liked to explore other decay processes : as the simulation stands now, only decays of the form $\phi\phi \rightarrow \rho \rightarrow \phi\phi$ can be studied. However, we could also study other structures where there is more than one decay product, or other variations on the same idea.

The physical model aside, this project has pieced together, pretty much from the ground up, a complicated interplay of C++ programs which run the simulation and other scripts which then analyze the data to extract meaningful data from the simulation. Careful thought has been put into optimizing not only the analysis portion of the process for speed by means of using Python, but also into speeding up the simulation itself. In this respect, future works include trying to implement an alternative update mechanism, using a two-level algorithm, which will allow for greater statistics to be achieved in shorter times.

Bibliography

- [1] Blossier et al. On the Generalized Eigenvalue Method for Energies and Matrix Elements in Lattice Field Theory. February 2009.
- [2] Chandler, David (1987). Introduction to Modern Statistical Mechanics. Oxford University Press.
- [3] Creutz, Michael (1985). Quarks, Gluons, and Lattices. Cambridge University Press.
- [4] Johnson, Charles (1990). Matrix Analysis. Cambridge University Press.
- [5] M. Luscher and U. Wolff. How to Calculate the Elastic Scattering Matrix in Two-Dimensional Quantum Field Theories by Numerical Simulations. Nucl. Phys. B339 (1990) 222
- [6] Rummukainen, K and Gottlieb, S. Resonance Scattering Phase Shifts on a Non-Rest Frame Lattice. March 1995.
- [7] Sakurai, J.J. (1994). Modern Quantum Mechanics. Addison-Wesley.